Korean Journal of Remote Sensing, Vol.26, No.3, 2010, pp.305~316

Comparison of Fusion Methods for Generating 250m MODIS Image

Sun-Hwa Kim †, Sung-Jin Kang, and Kyu-Sung Lee

Inha University, Dept. of Geoinformatic Engineering, Yonghyun-dong, Nam-ku, Incheon 402-751, KOREA

Abstract : The MODerate Resolution Imaging Spectroradiometer (MODIS) sensor has 36 bands at 250m, 500m, 1km spatial resolution. However, 500m or 1km MODIS data exhibits a few limitations when low resolution data is applied at small areas that possess complex land cover types. In this study, we produce seven 250m spectral bands by fusing two MODIS 250m bands into five 500m bands. In order to recommend the best fusion method by which one acquires MODIS data, we compare seven fusion methods including the Brovey transform, principle components algorithm (PCA) fusion method, the Gram-Schmidt fusion method, the least mean and variance matching method, the least square fusion method, the discrete wavelet fusion method, and the wavelet-PCA fusion method. Results of the above fusion methods are compared using various evaluation indicators such as correlation, relative difference of mean, relative variation, deviation index, peak signal-to-noise ratio index and universal image quality index, as well as visual interpretation method. Among various fusion methods, the local mean and variance matching method provides the best fusion result for the visual interpretation and the evaluation indicators. The fusion algorithm of 250m MODIS data may be used to effectively improve the accuracy of various MODIS land products.

Key Words : MODIS, Fusion, Resolution, Evaluation index, LMVM, spectral preservation, PSNR.

1. Introduction

Since the launching of the Terra and Aqua satellite of EOS(Earth Observing System) project, the Moderate Resolution Imaging Spectrometer(MODIS) has delivered global scale atmospheric, terrain- and ocean- biophysical products. The MODIS sensor has a total of 36 spectral bands that is composed of two 250m spatial resolution bands, five 500m bands, and twenty nine 1km bands (Sirguey *et al.*, 2008; Luo *et al.*, 2008). Most MODIS biophysical products are provided at 1 km spatial resolution. However, there are some limitations in using 500m or 1km spatial resolution MODIS data for small areas that possess complex land cover types, such as the Korean Peninsula (Kim and Lee, 2003; Kim, 2003). The low spatial resolution of MODIS data often decreases the accuracy of global MODIS products as Snow cover (MOD10), Land cover (MOD12), Thermal anomalies (MOD14), and LAI/FPAR (MOD15) (Sirguey *et al.*,

Received May 20, 2010; Revised June 18, 2010; Accepted June 23, 2010.
† Corresponding Author: Sun-Hwa Kim (rssun@inha.ac.kr)

2008; 2009; Kim and Lee, 2003; Kim, 2003; Kim *et al.*, 2009; Tian *et al.*, 2000; Wang *et al.*, 2001). It is important and desired to have all 500m bands at the 250m spatial resolution for providing detailed spectral and spatial information about various land cover types(Luo *et al.*, 2008). A few previous studies exist concerning the improvement of spatial resolution of MODIS data. It is attempted the wavelet-based image fusion of two 250m bands and five 500m bands based on the high correlation between 250m bands and 500m bands (Sirguey *et al.*, 2008; 2009). In another study, an adaptive regression model between 500m bands and 250m band 1, 2, NDVI(Trishchenko *et al.*, 2006; Luo *et al.*, 2008) is used. These 250m fused dataset are useful in producing a more accurate snow map or radiance product at an improved 250m spatial resolution (Sirguey *et al.*,2008; 2009; Luo *et al.*, 2008). However, the wavelet fusion method shows lower visual interpretation. Additionally, an adaptive regression model method requires many processing steps and time because of using all MODIS pixels (Kim *et al.*, 2009; Buntilov and Bretschneider, 2007; Luo *et al.*, 2008). This MODIS fusion is different from the general pan-sharpening or fusion cases at two aspects. First is that MODIS has no panchromatic band. Instead of the panchromatic band, 250m MODIS band 1(Red), 2(NIR) are used in this study. There are also the disagreement of the spectral wavelength between the high resolution and low resolution images. The other is that MODIS fusion shows the different fusion method of the multi-high resolution images and multi-low resolution images comparing with the general method fusing one high resolution to multi-low resolution image. For solving two MODIS fusion problems, we suggest the best band combination of high and low resolution MODIS bands. Using this best MODIS band combination, we apply seven standard fusion methods and recommend the best fusion method for generating 250m MODIS data.

2. Methods

1) Dataset used

The MODIS radiance data (MOD02) used in this study was obtained by an EOS Terra satellite in April 5, 2005. The MODIS data was obtained over various land covered regions in the central part of the Korean peninsula as Fig. 1. In this study, we used only the two 250m bands and five 500m bands over a reflected wavelength area. Although there is the general fusion method of fusing one high-resolution image to multiple low-resolution images, two MODIS high resolution images and five MODIS low resolution images are fused in this study, as shown in Table 1. Because the fusion result is related to the spectral similarity of the high and low resolution images, it is necessary to choose the best band combination (Table 1). To achieve a good band combination, we analyze the statistics and histogram of the MODIS bands, as shown in Tables 2, 3 and Fig. 2. In Tables 2 and 3, B1 (red) shows a higher correlation to B3 (blue), and B4 (green) and B2 (NIR) are correlated to B4(NIR), B5(NIR),

Table 1. Dataset used

Item	Specification	
Sensor	Terra MODIS	
Date	April 5, 2005 (A.M. 10:30)	
Fusion data	High-resolution band (250m)	Low-resolution band (500m)
	Band 1 (0.645 μm)	Band 3 (0.469 μm) Band 4 (0.555 μm)
	Band 2 (0.858 μm)	Band 5 (1.24 μm) Band 6 (1.64 μm) Band 7 (2.13 μm)
Image size	1242C * 847R	622C * 424R

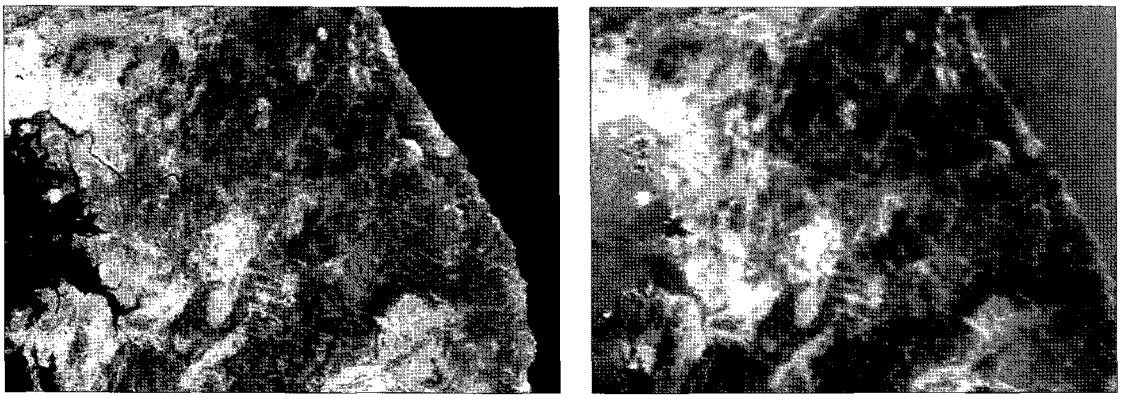

Fig. 1. MODIS 250m band 1(left) and 500m color composite image (right).

Table 2. 1st statistics of Terra MODIS data on April 5, 2005 (unit: W/m2/sr/um)

Bands	Mean	Std.	Min	Max
Band 1(Red)	2,048.041	292.718	0	8,605
Band 2(NIR)	3,890.889	932.338	0	20,613
Band 3(Blue)	4,779.586	356.356	0	6,329
Band 4(Green)	3,733.989	367.856	0	5,998
Band 5(NIR)	3,587.788	1,213.433	0	7,496
Band 6(SWIR)	3,555.351	1,392.923	0	8,828
Band 7(SWIR)	2,999.612	1,269.314	0	9,940

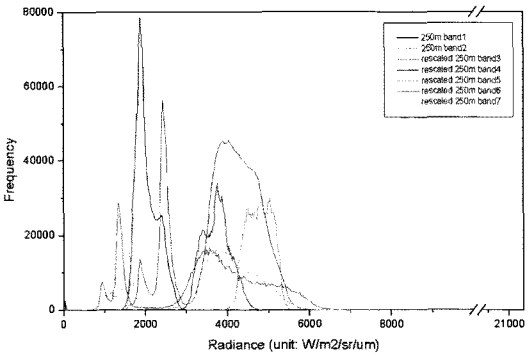

Fig. 2. Histogram of MOD02 seven bands.

B6(SWIR) and B7(SWIR). In Fig. 2, the histograms of visible wavelength bands show one peak distribution and infrared wavelength bands show the three peak distributions. Using the spectral similarity between bands, the 250m band 1 (red) and 500m band 3 (blue), 4 (green) were fused, and 250m band 2 (NIR) and 500m MODIS band 5 (NIR), 6 (SWIR), 7 (SWIR) were fused.

2) Image fusion methods

The purpose of this study, with regards to MODIS fusion, is to generate sharpened images while preserving spectral information. In order to recommend the best MODIS fusion method, we applied and compared a total seven various fusion algorithms used in various pan-sharpening fusion

Table 3. Correlation between bands of Terra MODIS data on April 5, 2005

Bands	**Band1**	**Band2**	Band3	Band4	Band5	Band6	Band7
Band 1(Red)	1.000	-	-	-	-	-	-
Band 2(NIR)	0.635	1	-	-	-	-	-
Band 3(Blue)	**0.577**	-0.050	1	-	-	-	-
Band 4(Green)	**0.502**	0.238	0.876	1	-	-	-
Band 5(NIR)	0.465	**0.927**	-0.174	0.141	1	-	-
Band 6(SWIR)	0.556	**0.910**	0.088	0.249	0.973	1	-
Band 7(SWIR)	0.637	**0.875**	0.014	0.361	0.930	0.981	1

cases. These fusion methods are composed of the colour transform fusion method (e.g. IHS fusion) and a statistical or numerical fusion method (e.g. PCA fusion).

(1) Brovey transform method: the Brovey transform fusion method was developed to visually increase contrast in the low and high ends of an image's histogram(Zhou *et al.*, 1998; Wang *et al.*, 2005;). Each band is multiplied by a ratio of the high resolution data divided by the sum of the low resolution bands as follows:

$$F_i = \frac{LR_i}{LR_1 + LR_2 + \cdots + LR_n} \times HR \qquad \text{(Eq.1)}$$

F_i: MODIS 250m fused image at i band
$LR_{1,2,\cdots n}$: MODIS 500m original bands
HR: MODIS 250m original band

Brovey transformation fusion is applied by ERDAS Imagine software.

(2) PCA fusion method: the Principle Component Algorithm (PCA) forward transform is applied to the low resolution multispectral image for generating principle components(Zhou *et al.*, 1998; Wang *et al.*, 2005). The high resolution image is substituted for PC-1 after which the PCA backward transform is performed. The PCA fusion method is good because the spectral information of the original low resolution image is retained after applying the fusion method (Karathanassi *et al.*, 2007). PCA fusion is applied by ERDAS Imagine software.

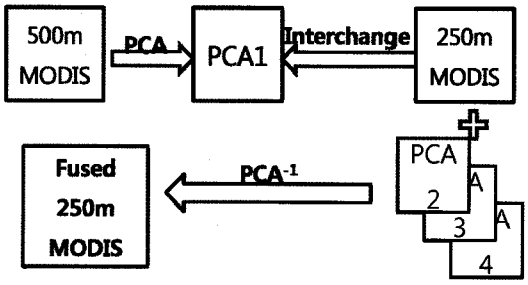

Fig. 3. PCA fusion algorithm.

(3) Gram-Schmidt fusion method: The main processing function of the Gram-Schmidt fusion method is similar to that of the PCA fusion method. A low resolution panchromatic image is simulated from a low resolution multispectral images by using empirical formulas. The Gram-Schmidt orthogonalization transform is performed on the simulated low resolution panchromatic image and the original low-resolution multispectral images. The high resolution image is substituted for first Gram-Schmidt image; then, the Gram-Schmidt backward transform is performed for image fusion. This fusion is run in ENVI software.

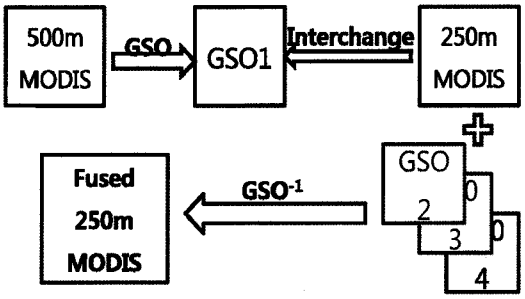

Fig. 4. Gram-Schmidt fusion algorithm.

(4) Local mean and variance matching method: LMVM filter requires the application of Equation 2 for the normalization between the high resolution and low resolution image using local mean and variance values of two target images. Using local statistics of high and low resolution images, the correlation between the fused image and the low resolution image is greater than other fusion methods (Karathanassi *et al.*, 2007). This fusion is run in ERDAS Imagine software.

$$F_{i,j} = \frac{(HR_{i,j} - \overline{HR_{i,j(w,h)}} \times std(LR)_{i,j(w,h)})}{std(HR)_{i,j(w,h)}} + \overline{LR_{i,j(w,h)}} \qquad \text{(Eq. 2)}$$

$F_{i,j}$: MODIS 250m fused image at pixel coordinates i, j
$H_{i,j}$: MODIS 260m original image at pixel coordinates i, j
$\overline{LR_{i,j(w,h)}}$: The local mean of MODIS 500m original image calculated inside the window of size (w, h) at pixel coordinates i, j

$\overline{HR}_{i,j(w,h)}$: The local mean of MODIS 250m original image calculated inside the window of size (w, h) at pixel coordinates i, j

$std(LR)_{i,j(w,h)}$: The local standard deviation of MODIS 500m original image calculated inside the window of size (w, h) at pixel coordinates i, j

$std(HR)_{i,j(w,h)}$: The local standard deviation of MODIS 250m original image calculated inside the window of size (w, h) at pixel coordinates i, j

(5) Least square fusion method: With LMVM fusion method, the LST fusion method is a standard statistical fusion method. This method approximates the grey value relationship between the high-resolution, low resolution, and fused images to generate a best colour representation using a least square method (Zhang, 2002). LST is applied by PCI Geomatica software.

(6) Wavelet fusion method: The wavelet transform decomposed the 250m MODIS data, and produced a set of detailed coefficients, as shown in Fig. 5 (Zhou *et al.*, 1998). These coefficients can be corrected by an adequate model before being injected in the 500m MODIS data to improve the quality of the synthesized image. The modified coefficients are used along with the 500m MODIS data for reconstruction, making the spatial resolution of the reconstructed image the same as that of the 250m data. Discrete wavelet fusion is run in Matlab code.

(7) Wavelet-PCA fusion method: This method combines the PCA and Wavelet fusion method (King and Wang, 2001). The wavelet fused image is substituted for PC-1 after which the PCA backward transform is performed. This fusion method produces fused images with less spectral distortion. (Karathanassi *et al.*, 2007). Discrete wavelet fusion is run in Matlab code.

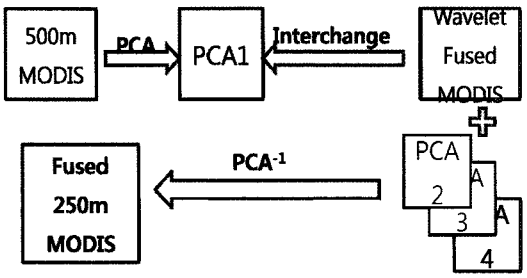

Fig. 6. Wavelet-PCA fusion method.

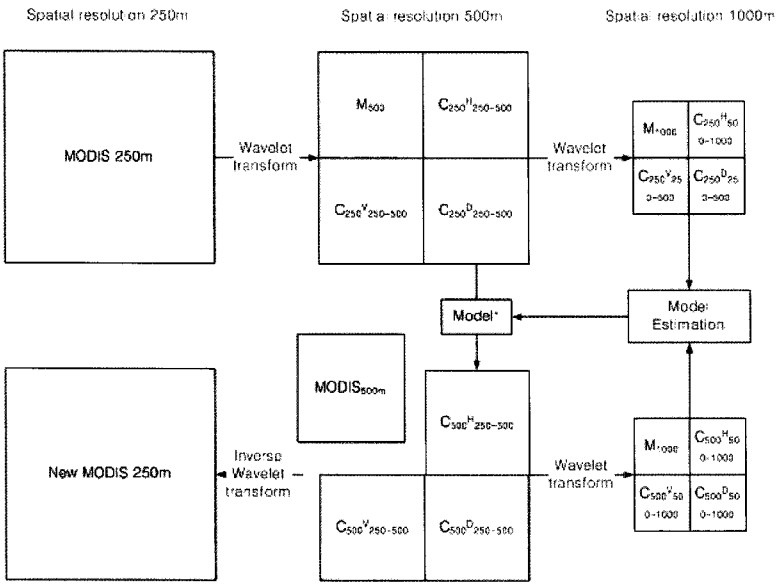

Fig. 5. MODIS wavelet fusion method.

3) Evaluation indicators

To validate the fused results, we used six statistical evaluation indicators with visual interpretations. In visual interpretation, the sharpness and colour tone of fused 250m MODIS images is analysed and compared with original 250m and 500m MODIS images. Evaluation indicators showed the degree of spectral preservation from fused data in comparison to the original image. Indicators, as presented in Table 4, are the correlation (Zhou *et al.*, 1998), relative difference of means, relative variation difference, deviation index measured the normalized global absolute difference, and the peak signal to noise ratio (PSNR) index (Li and Hu, 2004) which revealed the radiometric distortion, and the Universal Image Quality Index(UQI) introduced by Wang and Bovic (2002) between the fused image and original 500m MODIS data. Table 4 shows various evaluation indicators, formulas, and relationships between the best means by which spectral information is preserved and an indicator value.

3. Results

To compare and assess the spectral and spatial

Table 4. Evaluation indicators of fused dataset

Indicator	Formula	Best spectral preservation
Correlation	$\gamma = \frac{Cov_{LR\text{-}F}}{\sigma_{LR}\sigma_F}$ 1)	Higher
Relative difference of means	$\frac{\bar{F}-\overline{LR}}{\overline{LR}}$ 2)	Smaller
Relative variation difference	$\frac{\sigma_F^2-\sigma_{LR}^2}{\sigma_{LR}^2}$ 3)	Smaller
Deviation index	$\frac{1}{R\times C}\sum_{i=1}^{R}\sum_{j=1}^{C}\frac{\lvert F_{i,j}-LR_{i,j}\rvert}{LR_{i,j}}$ 4)	Smaller
Peak signal to noise ratio index (PSNR)	$MSE=\frac{1}{N}\sum_{i=1}^{N}(F_{i,j}-LR_{i,j})^2$ 5) $PSNR=20\log_{10}\frac{Peak}{\sqrt{MSE}}$ 6)	Higher
Universal Image Quality Index (UQI)	$Q=\frac{\sigma_{F\cdot LR}}{\sigma_F\sigma_{LR}}\frac{2\bar{F}\overline{LR}}{(\bar{F})^2+(\overline{LR})^2}\frac{2\sigma_F\sigma_{LR}}{\sigma_F^2+\sigma_{LR}^2}$ 7)	Higher

1) Cov_(LR-F) : Covariance of MODIS 500m original and 250m fused image
1), 3), 7) σ_LR : standard deviation of MODIS 500m original image
1), 3), 7) σ_F : standard deviation of MODIS 250m fused image
2), 7) $\bar{F}$: the mean value of the MODIS 250m fused image
2), 7) $\overline{LR}$: the mean value of the MODIS 500m original image
4) R: row of image
4) C: column of image
4), 5) $F_{i,j}$:MODIS 250m fused image at pixel coordinates i, j
4), 5) $\mathbf{LR_{i,j}}$: MODIS 500m original image at pixel coordinates i, j
5) N: the number of non-null image pixels
5) Peak: the maximum possible pixel value, Peak is 65,535 for 16bits

quality of seven MODIS fusion methods, we evaluated the fused results using visual interpretation and various statistical evaluation indicators. For obtaining visual interpretation results, as shown in Fig. 7 and 8, we evaluated the improvement of spatial resolution and spectral fidelity. In comparison to the original 500m MODIS image, the spatial resolution of 250m fused images is increased. The sharpest fusion products are obtained by the LMVM (local mean and variance matching) method. On the other

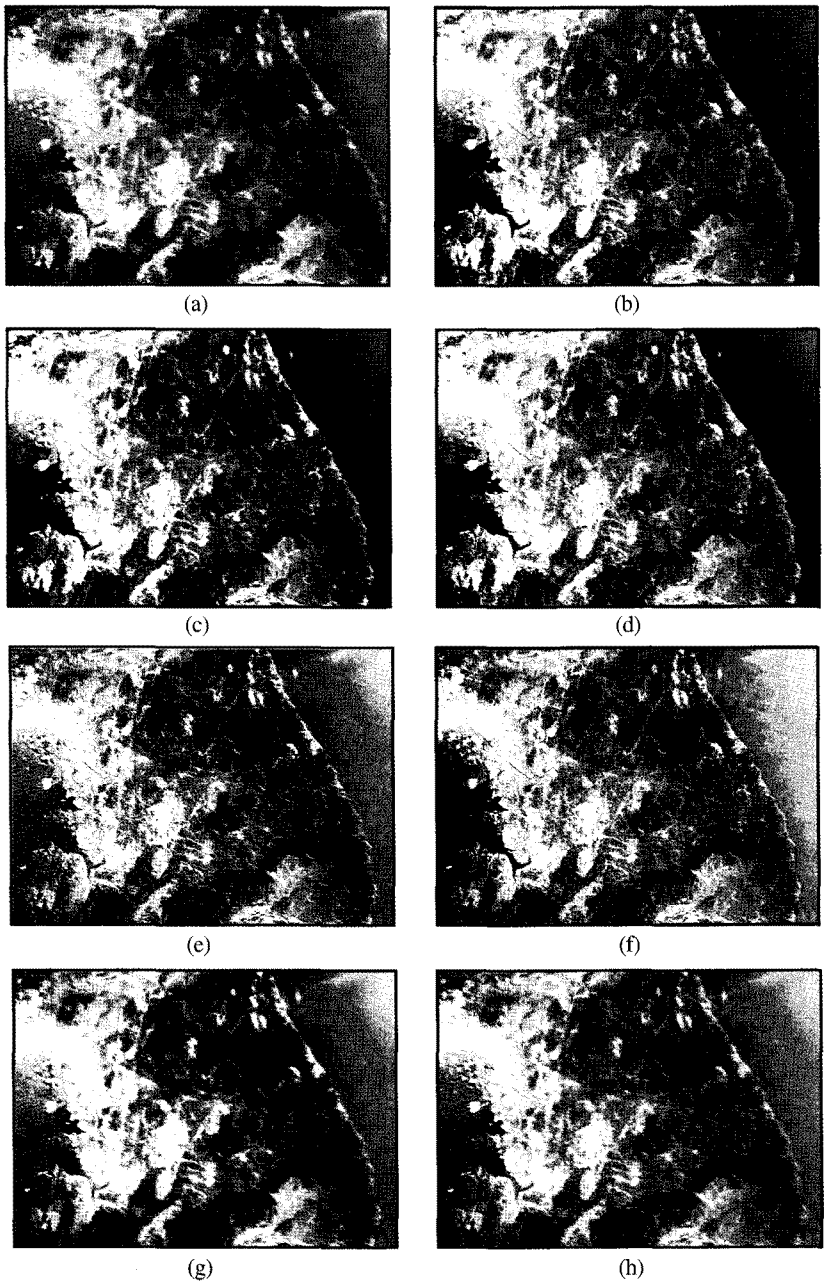

Fig. 7. Original MODIS 500m image (a), Brovey transform fusion image (b), PCA transform fusion image (c), Gram-Schmidt fusion image (d), LMVM fusion image (e), LST fusion image (f), Wavelet fusion image (g), Wavelet-PCA fusion image (h).

hand, the fused images acquired after using wavelet-based fusion methods and the wavelet-PCA fusion method show a sharpness slightly less than the fused images acquired through the LMVM method. The degradation, or distortion, of the images obtained from the wavelet fusion methods increased as the dissimilarity of the spectral responses of the high and low spatial resolution dataset increased (Buntilov and Bretschneider, 2007). Therefore, the wavelet fusion method may be unsuitable for MODIS data possessing spectral differences. When analysing the colour tone of the fusion results, the colour composited images produced after the employment of the PCA and Gram-Schmidt fusion algorithms exhibited different colour tones in comparison to the original colour composited image. LMVM fusion results exhibited a similar colour tone as the original MODIS data.

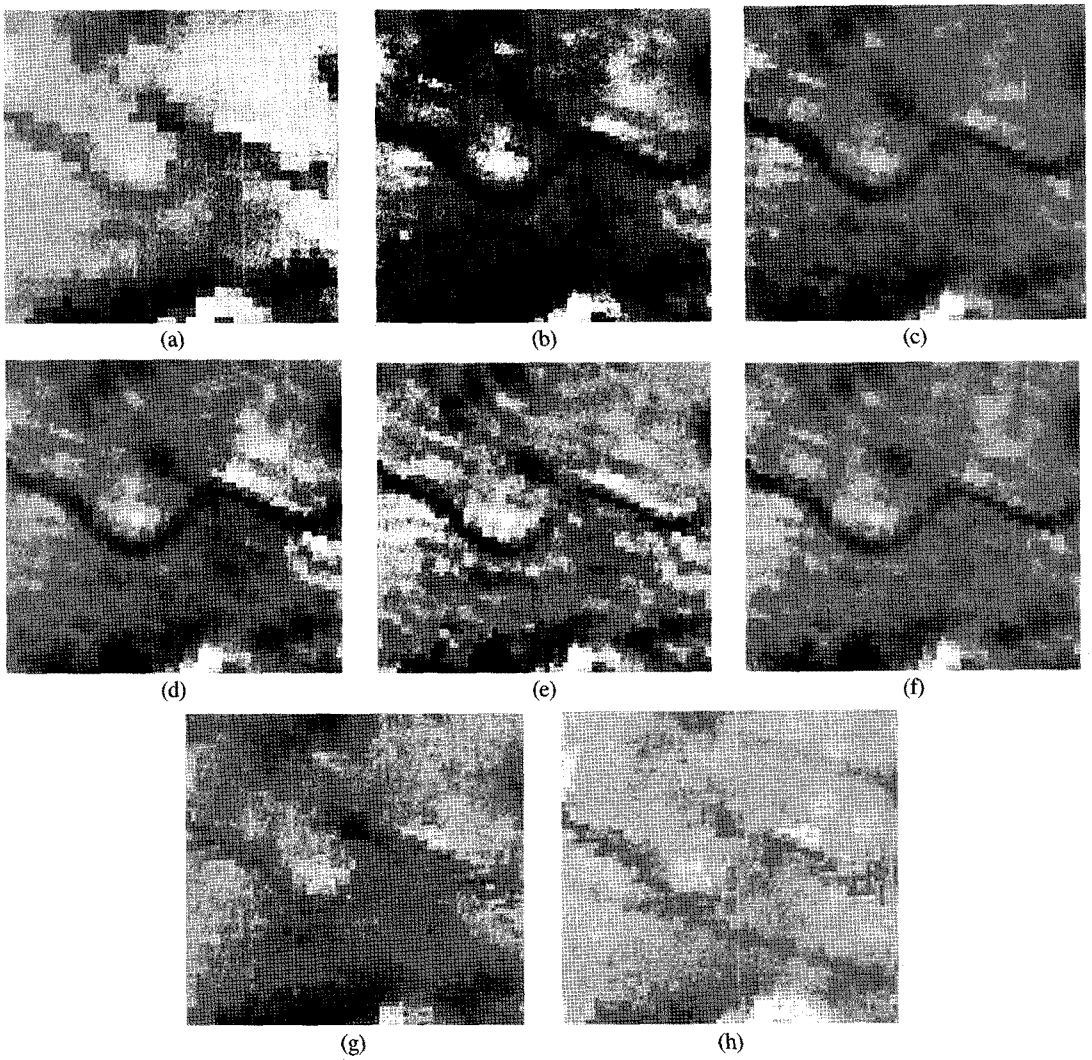

Fig. 8. Subset images of original 500m (a), Brovey transform fusion image (b), PCA fusion image (c), Gram-Schmidt fusion image (d), LMVM image (e), LST fusion image (f), wavelet fusion image (g), and wavelet-PCA fusion image (h) on Han River area (74C * 68R).

Table 10 shows the average spectral fidelity of the fused 250m MODIS dataset in comparison to the original MODIS 500m bands. Of all of the MODIS fusion results, as shown in Table 10, the LST, PCA, and LMVM fusion methods showed the highest spectral fidelity and best preserved spectral information of original MODIS image. For a more detailed analysis, we analysed the spectral fidelity of each MODIS band, summarized in Tables 5~9. The fusion method possessing higher spectral fidelity is different on each spectral band. PCA fusion results showed a high spectral fidelity in the MODIS band

Table 5. Spectral fidelity of MODIS band 1(Red)-band 3(Blue) fusion results

B1-B3	Bro	**PCA**	Gram	LST	Wavelet	LMVM	W+PCA
Corr.	0.972	0.900	0.970	0.572	1.000	0.645	0.623
RDM	0.785	**-0.033**	-0.572	-0.572	-0.750	-0.381	-0.571
RVD	2.823	1.445	-0.166	**-0.041**	-0.500	-0.571	-0.333
DI	0.777	**0.071**	0.574	0.573	0.500	0.572	0.572
PSNR	37.115	**51.727**	27.594	27.536	28.731	27.558	27.588
UQI	0.000053	0.000104	0.000048	0.000070	0.000002	0.000058	0.000025

Table 6. Spectral fidelity of MODIS band 1(Red)-band 4(Green) fusion results

B1-B4	Bro	PCA	Gram	**LST**	Wavelet	LMVM	**W+PCA**
Corr.	0.982	0.944	0.984	0.914	1.000	0.848	0.849
RDM	1.278	1.376	-0.451	-0.452	-0.750	**-0.401**	-0.450
RVD	3.155	0.661	-0.437	**-0.361**	-0.500	-0.451	**-0.383**
DI	1.279	1.481	**0.454**	**0.455**	0.500	0.453	**0.451**
PSNR	**35.053**	**34.819**	31.770	31.738	30.858	31.737	31.791
UQI	0.000037	0.000027	0.000059	0.000069	0.000000	0.000056	0.000002

Table 7. Spectral fidelity of MODIS band 2(NIR)-band 5(NIR) fusion results

B2-B5	Bro	**PCA**	Gram	LST	Wavelet	LMVM	W+PCA
Corr.	0.503	0.258	0.495	0.590	1.000	0.545	0.495
RDM	0.717	**0.035**	-0.430	-0.431	-0.750	-0.931	-0.428
RVD	-0.557	-0.597	-0.936	-0.931	-0.500	**-0.430**	-0.922
DI	1.373	**0.244**	0.459	0.433	0.500	0.418	0.457
PSNR	36.697	**42.483**	30.727	30.898	30.776	30.868	30.826
UQI	0.000022	0.000039	0.000013	0.000014	0.000004	0.000014	0.000015

Table 8. Spectral fidelity of MODIS band 2(NIR)-band 6(SWIR) fusion results

B2-B6	Bro	PCA	**Gram**	**LST**	Wavelet	**LMVM**	W+PCA
Corr.	0.961	0.979	0.994	0.976	1.000	0.886	0.929
RDM	2.280	1.329	**0.092**	**0.091**	-0.750	-0.507	0.098
RVD	2.396	3.693	-0.519	-0.514	-0.500	**0.092**	-0.442
DI	3.126	1.342	0.255	**0.233**	0.500	**0.227**	0.278
PSNR	27.578	29.172	**41.396**	40.861	30.705	38.620	39.184
UQI	0.000007	0.000015	0.000017	0.000017	0.000004	0.000017	0.000018

Table 9. Spectral fidelity of MODIS band 2(NIR)-band 7(SWIR) fusion results

B2-B7	Bro	PCA	**Gram**	**LST**	Wavelet	**LMVM**	W+PCA
Corr.	0.935	0.843	0.978	0.936	1.000	0.849	0.897
RDM	2.892	1.980	**0.294**	**0.292**	-0.750	-0.401	0.302
RVD	3.254	4.261	-0.395	-0.411	-0.500	0.294	-0.324
DI	3.902	2.059	0.477	**0.441**	0.500	**0.429**	0.475
PSNR	26.978	27.833	**36.732**	36.241	32.086	35.419	35.648
UQI	0.000006	0.000010	0.000016	0.000016	0.000003	0.000016	0.000017

Table 10. Average spectral fidelity of all MODIS fusion results

	Bro	**PCA**	Gram	**LST**	Wavelet	**LMVM**	W+PCA
Corr.	0.870	0.785	0.884	0.798	**0.999**	0.755	0.759
RDM	1.590	0.937	**-0.213**	**-0.214**	-0.750	-0.524	**-0.210**
RVD	2.214	1.893	-0.491	-0.451	-0.500	**-0.213**	-0.481
DI	2.091	1.039	0.444	**0.427**	0.500	**0.420**	0.447
PSNR	32.684	**37.207**	33.644	33.455	30.631	32.840	33.007
UQI	0.000025	0.000039	0.000030	0.000037	0.000003	0.000032	0.000016

3(Blue) and 5 (NIR) fusion results, as shown in Tables 5 and 7. The Gram-Schmidt fusion method showed a high spectral fidelity in the MODIS band6 (SWIR) and band7 (SWIR) fused images, as shown in Tables 8 and 9. For the fusion of the MODIS band 4 (Green), the LST and LMVM methods showed good spectral fidelity, as shown in Table 6. The negative value of RDM or RVD means that statistics of MODIS fused data is higher than MODIS 500m original value. The absolute value of RDM or RVD is important for analysing the spectral fidelity of MODIS original and fused dataset. The fused results for each MODIS band are different because of the spectral wavelength disagreement between MODIS 250m bands (high spatial resolution image) and 500m bands (low spatial resolution image). Consequently, difficulty arises when recommending one powerful fusion method. Although various fusion methods exhibited rather lower spectral fidelity, all fusion results displayed an improvement in the spatial resolution in comparison to the MODIS original image.

4. Conclusions and discussions

The usage limitations of MODIS data comprising low spatial resolution for land monitoring was presented. In this study, we attempted to fuse 250m and 500m MODIS data using seven fusion methods for improving the spatial resolution of MODIS data. To compare and validate various MODIS fusion methods, we analysed visual interpretation results of a fused dataset and six statistical evaluation indexes showing the spectral fidelity of the fused data. After comparing the results of the fused dataset, the following conclusions were developed:

- From the visual interpretation results, it was seen that major fusion methods exhibited a higher spatial resolution than the 500m MODIS original image. However, the Wavelet fusion method exhibited blurred fusion results, and the PCA method displayed a different colour tone in comparison to the 500m MODIS original image.
- From the spectral fidelity results in which various evaluation indexes were utilized, the LST, PCA, and LMVM fusion methods demonstrated a

relatively high degree of spectral preservation of original MODIS data. However, different results for each MODIS band or wavelength area exist. This phenomenon may be caused by the spectral wavelength disagreements between the 250m MODIS data and the 500m MODIS data.

- Among various fusion methods, the LMVM fusion method showed the best fusion results in spatial resolution and spectral fidelity.
- 250m fused MODIS dataset possessing a sharper image and higher spectral fidelity than the original MODIS dataset may be useful in generating more accurate MODIS land products.
- In future studies, we will develop more powerful fusion methods that resolve wavelength disagreement of MODIS data.

Acknowledgements

This research was supported by a grant (07KLSGC03) from Cutting-edge Urban Development - Korean Land Spatialization Research Project funded by Ministry of Land, transport and Maritime Affairs of Korean government.

References

Buntilov, V. and Bretschneider, T. R., 2007. A concept separation image fusion approach: Toward conformity between spectral and spatial information, *IEEE Transactions on Geoscience and Remote Sensing*, 45(10): 3252-3263.

Karathanassi, V., Kolokousis, P., and Ioannidou, S., 2007. A comparison study on fusion methods using evaluation indicators, *International Journal of Remote Sensing*, 28(10): 2309-2341.

Kim, S. H. and Lee, K. S., 2003. Local validation of MODIS Global leaf area index (LAI) product over temperate forest, *Korean Journal of Remote Sensing*, 19(1):1-9

Kim, S. H., 2003. Validation of MODIS Leaf Area Index product at temperate forest in Central Korea, Master's Thesis, Inha University, Republic of Korea.

Kim, S. H., Kang S. J., and Lee K. S., 2009. Comparison of the fusion methods for generating of 250m MODIS data, *KSRS Spring conference 2009*.

King, R. and Wang, J., 2001. A wavelet based algorithm for pan sharpening Landsat 7 imagery, *International Geoscience and Remote Sensing Symposium*, 2: 849-851.

Li, Q. and Hu Q., 2004. 3D wavelet compression to multiple band remote sensing images based on edge reservation, *Proceedings of the ISPRS*, Commission VII, Istanbul 2004, Published on CD-Rom, paper no.11.

Luo, Y., Trishchenko A. P., and Khlopenkov K. V., 2008. Developing clear-sky, cloud and cloud shadow mask for producing clear-sky composites at 250-meter spatial resolution for the seven MODIS land bands over Canada and North America, *Remote Sensing of Environment*, 112: 4167-4185.

Pohl, C. and Van Genderen, J. L., 1997. Multisensor image fusion in remote sensing: concepts, methods and applications, *International Journal of Remote Sensing*, 19: 823-854.

Sirguey, P., Mathieu, R., Arnaud, Y., Khan, M., and Chanussot, J., 2008. Improving MODIS spatial resolution for snow mapping using wavelet fusion and ARSIS concept, *IEEE Geoscience and Remote sensing letters*, 5(1): 78-82.

Sirguey, P., Mathieu, R., and Arnaud, Y., 2009. Subpixel monitoring of the seasonal snow cover with MODIS at 250m spatial resolution in the Southern Alps of New Zealand: Methodology and accuracy assessment, *Remote Sensing of Environment*, 113: 160-181.

Tian, Y., Zhang, Y., and Knyazikhin, Y., 2000. Prototyping of MODIS LAI and FPAR algorithm with LASIR and Landsat data, *IEEE Transactions on Geoscience and Remote Sensing*, 38: 2387-2400.

Trishchenko, A. P., Luo, Y., and Khlopenkov, K. V., 2006. A method for downscaling MODIS land channels to 250m spatial resolution using adaptive regression and normalization, *Proceedings of SPIE-The International Society for Optical Engineering*, 6366(636607): 8.

Wang, Y., Tian, Y., and Zhang, T., 2001. Invegetation of product accuracy as a function of input an model uncertainties case study with SeaWiFS and MODIS LAI/FPAR algorithm, *Remote Sensing of Environment*, 78: 299-313.

Wang, Z. and Bovic, A. C., 2002. A University Image Quality Index, *IEEE Signal Processing Letters*, 9: 81-84.

Wang, Z. Ziou, D., Armenakis, C., Li, D., and Li, Q., 2005. A comparative analysis of image fusion methods, *IEEE Transactions on Geoscience and Remote Sensing*, 43(6): 1391-1402.

Zhang, Y., 2002. Problems in the fusion of commercial high-resolution satellite images as well as Landsat 7 images and initial solutions, *International Archives of Photogrammetry and Remote Sensing (IAPRS)*.

Zhou, J., Civco, D. L., and Silander, J. A., 1998. A wavelet transform method to merge Landsat TM and SPOT panchromatic data, *International Journal of Remote Sensing*, 19(4): 743-757.